

Spontaneous symmetry emergence in a Hermitian system without symmetry

T. T. Sergeev, E. S. Andrianov, and A. A. Zyablovsky*

*Dukhov Research Institute of Automatics, 127055, 22 Sushchevskaya, Moscow, Russia
Moscow Institute of Physics and Technology, 141700, 9 Institutskiy pereulok, Moscow, Russia and
Institute for Theoretical and Applied Electromagnetics, 125412, 13 Izhorskaya, Moscow, Russia*

(Dated: April 30, 2024)

Spontaneous symmetry breaking in systems with symmetry is a cornerstone phenomenon accompanying second-order phase transitions. Here, we predict the opposite phenomenon, namely, spontaneous symmetry emergence in a system without symmetry. On the example of two coupled oscillators interacting non-symmetrically with a set of oscillators whose frequencies uniformly fill a finite frequency range, we demonstrate that the system state can acquire symmetry, which is not inherent to the system Hamiltonian. The emergence of symmetry manifests itself in a change of the system dynamics, which can be interpreted as a phase transition in a Hermitian system without symmetry.

I. INTRODUCTION

Spontaneous symmetry breaking is a key concept in physics [1–4] and is used for the description of second-order phase transitions [1–4]. Conventionally, phase transitions are studied in closed systems described by Hermitian Hamiltonians [5]. It is known [5] that if the linear Hermitian operator commutes with any other linear Hermitian operator, then one can find a system of eigenstates that is common to both operators. Therefore, if the system Hamiltonian has symmetry, i.e., commutes with the symmetry operator, then there is a basis of eigenstates that are also eigenstates of the symmetry operator [5]. A phase transition occurs when the symmetry of the instantaneous state of the system becomes lower than the Hamiltonian symmetry, which is possible when the ground state of the system is degenerate [5]. In this case, the spontaneous symmetry breaking means a decrease in the symmetry of the instantaneous state of the system [1], though the symmetry of the eigenstates coincides with the Hamiltonian symmetry.

In recent decades, it has been shown that in non-Hermitian systems, it is possible that the symmetry of the eigenstates is lower than the symmetry of the system Hamiltonian [6–8]. As a result, one can observe another type of spontaneous symmetry breaking [8–12], which manifests as the decrease of the symmetry of eigenstates with simultaneous conservation of the Hamiltonian symmetry. This type of spontaneous symmetry breaking is associated with non-Hermitian phase transitions [13–20]. PT-symmetrical systems are one of the most famous examples of systems with this type of spontaneous symmetry breaking [15, 16]. In these systems, the change in the system parameters leads to passing through an exceptional point (EP) [15, 16], at which the eigenstates cease to be PT-symmetrical, whereas the Hamiltonian is still PT-symmetrical. In addition to PT-symmetrical systems, non-Hermitian phase transitions can also occur

in strongly coupled cavity-atom systems [15, 21], polariton [22, 23], optomechanical [24–29], and laser [30–34] systems. The systems with the phase transitions at the EP find a number of the applications [35–40].

However, a consistent description of the phase transitions at the EPs encounters difficulty. Indeed, any non-Hermitian system is actually subsystem of a larger Hermitian system, consisting of the considered non-Hermitian system and its environment. The transition from a Hermitian description to a non-Hermitian one is carried out by elimination of the environment's degrees of freedom, in particular, in the Born-Markovian approximation. The presence of the symmetry in the resulting non-Hermitian system does not guarantee that the original Hermitian system has the same symmetry. That is, the symmetry of a non-Hermitian system and its eigenstates may be a consequence of the inaccuracy of non-Hermitian description. Consequently, the spontaneous symmetry breaking of eigenstates can also be a consequence of the inaccuracy of the non-Hermitian consideration.

An Hermitian system that describe PT-symmetry breaking after elimination reservoir's degrees of freedom is a system consisting of two coupled oscillators and a set of oscillators interacting with one of the coupled oscillators. Such a Hermitian system is not symmetric with respect to the permutation of the first and second oscillators. However, if we exclude from consideration the degrees of freedom of the oscillators in the set then the resulting non-Hermitian system will be quasi-PT-symmetrical [10]. The eigenstates of such a non-Hermitian system are PT-symmetrical when the coupling strength between the oscillators is greater than a threshold value. Below the threshold values, the eigenstates are not PT-symmetrical and therefore a spontaneous breaking of PT-symmetry of the eigenstates occurs at the threshold value of coupling strength. However, since symmetry is not inherent in the initial system, it is unclear whether spontaneous symmetry breaking is associated with any change in the Hermitian system.

Here, we demonstrate that in the Hermitian system that is not symmetrical with respect of permutation of its

* zyablovskiy@mail.ru

elements the phenomenon opposite to spontaneous symmetry breaking, namely, spontaneous symmetry emergence takes place. On the example of two harmonic oscillators on which interacts with the set of large number of harmonic oscillators, we show that an increase in the coupling strength between the oscillators leads to the emergence of symmetry with respect to the permutation of the first and second oscillators in the dynamics of the Hermitian system. We demonstrate that there is a critical coupling strength above which the average absolute amplitudes of the first and second oscillators become equal to each other. This is associated with the appearance of a sharp threshold and is a manifestation of a new phenomenon that can be called spontaneous symmetry emergence. Thus, we predict the existence of a spontaneous symmetry emergence that takes place in the system, which does not possess emergent symmetry.

The critical coupling strength coincides with the one, at which the splitting in the spectrum of the quasi-PT-symmetrical system appears. Based on them, we can assume that spontaneous symmetry emergence in the Hermitian systems can be an initial cause of the changing of symmetry in the non-Hermitian systems. We believe that the spontaneous symmetry emergence serves as a source for a phase transitions in a Hermitian systems without symmetry.

II. SYSTEM UNDER CONSIDERATION

We consider a Hermitian system consisting of two coupled oscillators and a set of N oscillators interacting with the first oscillator [Figure 1]. The two main oscillators have equal frequencies, ω_0 . The frequencies of oscillators in the set are $\omega_k = \omega_0 + \delta\omega (k - N/2)$, where k is a number of the oscillators and $\delta\omega \ll \omega_0$ is a distance between the frequencies of the oscillators. In the experiment, this system can be realized, for example, on the basis of an optical structure of two coupled single-mode cavities, one of which interacts with a waveguide of finite length. Due to the finite length of the waveguide, its modes have a discrete set of frequencies, the specific values of which are determined by the frequency dispersion and geometry of the waveguide.

We use the following Hamiltonian for the system [41]:

$$\hat{H} = \omega_0 \hat{a}_1^\dagger \hat{a}_1 + \omega_0 \hat{a}_2^\dagger \hat{a}_2 + \Omega (\hat{a}_1^\dagger \hat{a}_2 + \hat{a}_2^\dagger \hat{a}_1) + \sum_{k=1}^N \omega_k \hat{b}_k^\dagger \hat{b}_k + \sum_{k=1}^N g (\hat{b}_k^\dagger \hat{a}_1 + \hat{a}_1^\dagger \hat{b}_k) \quad (1)$$

where $\hat{a}_{1,2}$ and $\hat{a}_{1,2}^\dagger$ are the annihilation and creation operators of the first and second oscillators, obeying the boson commutation relations $[\hat{a}_i, \hat{a}_j^\dagger] = \delta_{ij} \hat{1}$, $i, j = 1, 2$ [41]. \hat{b}_k and \hat{b}_k^\dagger are the annihilation and creation operators of the oscillators in the set with the frequencies ω_k . Ω is a coupling strength between the first and second oscillators; g is a coupling strength between the first oscillator

and each of the oscillators in the set. Note that we use the rotating-wave approximation to describe the interaction between oscillators [41].

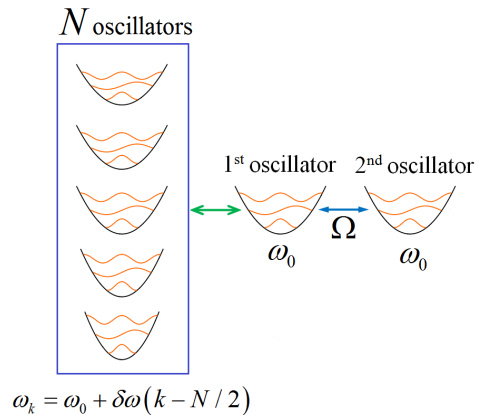


FIG. 1. The scheme of the system under consideration.

There are several approaches to studying the dynamics of the system (1). One approach was proposed in the work of Caldeira and Leggett [42] and is based on the study of the total density matrix using the Feynman-Vernon functional integral [42–44]. Another approach is to use Heisenberg equations for the operators [45, 46]. In our case, the last approach is more suitable because it enables us to consider the oscillators' amplitudes without additional approximations. Using the Heisenberg equation for operators [45, 46], we obtain a closed system of equations for operators $\hat{a}_{1,2}$, \hat{b}_k . Then moving from the operators to their averages, we obtain the linear system of equations (see Appendix A for more details)

$$\frac{da_1}{dt} = -i\omega_0 a_1 - i\Omega a_2 - i \sum_{k=1}^N g b_k \quad (2)$$

$$\frac{da_2}{dt} = -i\omega_0 a_2 - i\Omega a_1 \quad (3)$$

$$\frac{db_k}{dt} = -i\omega_k b_k - i g a_1 \quad (4)$$

where $a_1 = \langle \hat{a}_1 \rangle$, $a_2 = \langle \hat{a}_2 \rangle$ and $b_k = \langle \hat{b}_k \rangle$.

III. NON-HERMITIAN DESCRIPTION OF THE SYSTEM

The interaction of the first oscillator with the set of oscillators leads to an energy exchange between them. When the step between the frequencies of oscillators in the set tends to zero ($\delta\omega/\omega_0 \rightarrow 0$) and the number of the oscillators in the set tends to infinity ($N \rightarrow \infty$ and

$N\delta\omega = \text{const}$), this energy exchange transforms into energy dissipation in the first oscillator. In this case, the degrees of freedom of the oscillators in the set can be eliminated from consideration with the aid of the Born-Markovian approximation [45, 46]. In this approach, the system dynamics are described by the stochastic non-Hermitian equation (see Appendices B and C):

$$\frac{d}{dt} \begin{pmatrix} a_1 \\ a_2 \end{pmatrix} = \begin{pmatrix} -i\omega_0 - \gamma & -i\Omega \\ -i\Omega & -i\omega_0 \end{pmatrix} \begin{pmatrix} a_1 \\ a_2 \end{pmatrix} + \begin{pmatrix} \xi \\ 0 \end{pmatrix} \quad (5)$$

where $\gamma = \pi g^2 / \delta\omega$ is an effective decay rate and ξ is noise term, the correlation function of which is determined by the fluctuation-dissipation theorem [41, 45, 46].

To describe the system behavior is often used the non-Hermitian equations (5) without noise term. The eigenvalues of the equations (5) without noise term are $\lambda_{\pm} = -\frac{\gamma}{2} - i\omega_0 \pm \frac{1}{2}\sqrt{\gamma^2 - 4\Omega^2}$ and the respective eigenstates have the form

$$\mathbf{e}_{\pm} = \left\{ i \left(-\gamma \pm \sqrt{\gamma^2 - 4\Omega^2} \right) / 2\Omega, 1 \right\}^T \quad (6)$$

In this non-Hermitian system, there is an exceptional point (EP) when $\Omega = \Omega_{EP} = \gamma/2$. At the EP, the eigenstates of non-Hermitian system become linearly dependent, and their eigenvalues are equal to each other [15]. When $\Omega < \Omega_{EP}$, the absolute values of the first and second components of each eigenstates are not equal to each other ($|\mathbf{e}_{\pm}|_1 \neq |\mathbf{e}_{\pm}|_2$) and the eigenstates (6) are not PT-symmetrical. In this case, the imaginary parts of the eigenvalues, which determine the oscillation frequencies of the eigenstates, are equal to each other. When $\Omega > \Omega_{EP}$, the absolute values of the first and second components of the eigenstates become equal to each other ($|\mathbf{e}_{\pm}|_1 = |\mathbf{e}_{\pm}|_2$) and the eigenstates (6) are PT-symmetrical [16]. In this case, the imaginary parts of the eigenvalues differ from each other. This indicates splitting in the system spectrum at the EP. The passing through the EP, occurring at the increase of coupling strength, is often associated with the spontaneous symmetry breaking in the eigenstates [10, 15].

The eigenstates can be symmetrical because the non-Hermitian system described by Eq. (5) is quasi-PT-symmetrical [10, 16]. It is seen that adding to the matrix on the right side of (5) the identity matrix multiplied by $\gamma/2$, we obtain the following matrix:

$$M = \begin{pmatrix} -i\omega_0 - \gamma/2 & -i\Omega \\ -i\Omega & -i\omega_0 + \gamma/2 \end{pmatrix} \quad (7)$$

which is PT-symmetrical [16]. Due to the fact that M is a non-Hermitian matrix, it is possible that the symmetry of the eigenstates is lower than the symmetry of the system matrix [7, 8]. As a result, one can observe spontaneous symmetry breaking in the eigenvectors [9, 10], when the

eigenvectors are PT-symmetrical at $\Omega > \Omega_{EP}$ and non-PT-symmetrical at $\Omega < \Omega_{EP}$. Adding the identity matrix does not change the eigenvectors of any matrix. Therefore, in the non-Hermitian system described by Eq. (5) the spontaneous symmetry breaking in the eigenstates is also observed. The transitions related with the spontaneous PT-symmetry breaking can occur in quantum [6, 47], optical [15, 16], magnonic [20, 23, 35, 48, 49], Bose-Einstein condensate [50–53] systems. These transitions manifest themselves in the system's dynamics. In particular, if the initial state of the system coincides with one of the eigenstates then the ratio of the absolute values of the amplitudes of the first and second oscillators averaged over time, $\langle |a_1| \rangle_t / \langle |a_2| \rangle_t$, becomes equal to 1 at $\Omega > \Omega_{EP}$ [see the dashed blue line in Figure 2], where $\langle |a_{1,2}| \rangle_t = \frac{1}{t_{max}} \int_0^{t_{max}} |a_{1,2}| dt$ and $t_{max} \rightarrow \infty$.

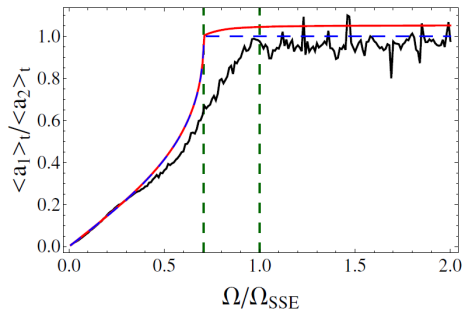


FIG. 2. The dependence of $\langle |a_1| \rangle_t / \langle |a_2| \rangle_t$ on the coupling strength Ω when the initial state has the form $a_1(t=0) = (\mathbf{e}_+)_{1}$, $a_2(t=0) = (\mathbf{e}_+)_{2}$ (see Eq. (6)), and $b_k(t=0) = 0$. The dashed blue line is calculated by the Eq. (5) and $t_{max} \rightarrow \infty$. The solid lines are calculated by the Eqns. (2)-(4) when $\langle |a_1| \rangle_t / \langle |a_2| \rangle_t$ is averaged over the time interval $0 \leq t \leq t_{max} = 0.5T_R$ (the red line) and $0 \leq t \leq t_{max} = 10T_R$ (the black line). The dashed vertical lines show $\Omega = \Omega_{EP} = \gamma/2$ and $\Omega = \Omega_{SSE} = \gamma/\sqrt{2}$.

The non-Hermitian description is only approximate, since it does not explicitly describe the behavior of the oscillators in the set. A complete description of the system is given by the Hermitian equations (2)-(4). However, in the Hermitian system there always is the system of the eigenstates, which have the same symmetries as the system Hamiltonian. Therefore, the spontaneous symmetry breaking cannot occur in the eigenstates of the Hermitian system. At the same time, the transitions with the change in symmetry are observed in the behavior of physical systems [15, 16], which actually are only subsystems of the Hermitian systems. Therefore, the question arises: what causes such transitions in Hermitian systems? In the following, we demonstrate that although the Hermitian system and its eigenstates are non-symmetrical for all values of Ω , there is a transition in which symmetry appears in the system dynamics.

IV. CHANGE IN EIGENSTATES OF THE HERMITIAN SYSTEM

Non-Hermitian equations correctly describe the system evolution only at $t \ll 2\pi/\delta\omega$. At longer times, $t \geq 2\pi/\delta\omega$, the Hermitian system demonstrates complex dynamics including collapses and revivals of the energy oscillations [44, 54–56], which arise at times greater than the return time $T_R = 2\pi/\delta\omega$ [55]. On this timescale, the system evolution is no longer described by the non-Hermitian equation (5) and is determined by the eigenfrequencies f_k and the eigenstates $\mathbf{e}_k = (e_k)_j$ ($j, k \in 1, \dots, N+2$) of the matrix on the right side of Eqns. (2)-(4).

The considered system (2)-(4) is Hermitian; thus, its eigenfrequencies are real and all eigenstates are mutually orthogonal. The variation of the coupling strength Ω leads to a change in the amplitudes of the components of the different eigenstates. We trace out the dependence of the amplitudes of the first and second components, $(e_k)_1$ and $(e_k)_2$, of the eigenstate \mathbf{e}_k on its eigenfrequency f_k [Figure 3]. These components correspond to the contributions of the first and second oscillators to the eigenstate \mathbf{e}_k . It is seen that the eigenstates do not possess symmetry with respect to the permutation of the first and second oscillators ($|(e_k)_1| \neq |(e_k)_2|$) at any values of Ω . This is due to the fact that the Hermitian system (2)-(4) is not symmetrical and the eigenstates of Hermitian systems always possess the same symmetry as the system. However, an increase in the coupling strength is still accompanied by a qualitative change in the behaviour of the eigenstates components.

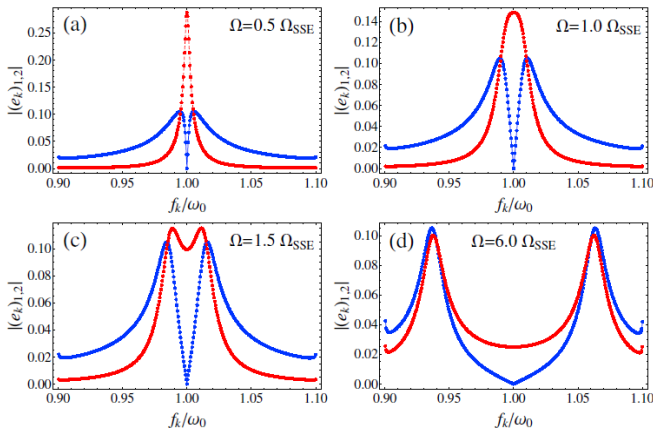


FIG. 3. The dependence of the amplitudes of the first $(e_k)_1$ (blue points) and second $(e_k)_2$ (red points) components in the eigenstate \mathbf{e}_k on its eigenfrequency f_k for the different coupling strengths: $\Omega = 0.5\Omega_{SSE}$ (a); $\Omega = \Omega_{SSE}$ (b); $\Omega = 1.5\Omega_{SSE}$ (c); $\Omega = 6.0\Omega_{SSE}$ (d). Here $\Omega_{SSE} = \gamma/\sqrt{2}$ and $\gamma = \pi g^2/\delta\omega$. The figures are plotted for $N = 400$.

At small values of the coupling strength, the value of the second component of the eigenstate with eigenfrequency $f_k = \omega_0$ is larger than the value of the second

component of any other eigenstates, see the peak of the red curve in Figures 3(a), (b). In contrast, this eigenstate with $f_k = \omega_0$ has a zero value of the first component [blue curves in Figures 3(a), (b)]. The increase in coupling strength leads to a splitting of the peak in the dependence of the second components of the eigenstates on their eigenfrequencies. This splitting begins to appear at the critical coupling strength $\Omega = \Omega_{SSE} = \gamma/\sqrt{2}$ [Figure 3(b), the red curve]. At $\Omega > \Omega_{SSE}$, some eigenstates with eigenfrequencies $f_k \neq \omega_0$ have the greatest value of the second components [the red curve in Figure 3(c)]. This reflects the fact that it is not the individual first oscillator that interacts with the set of oscillators but rather the coherent superposition of the first and second oscillators. At an increase in coupling strength above the critical value, the dependencies of the first and second components of the eigenstates on the eigenfrequencies f_k begin to become similar to each other [cf. the red and blue curves in Figures 3(c), (d)]. Thus, the qualitative change in the eigenstates occurs at $\Omega = \Omega_{SSE}$. When $N \gg 1$, such a change in the eigenstates of the Hermitian system does not depend on N (see Appendix E). Moreover, this change occurs even when the number of oscillators is about 10. That is, the change in the eigenstates is a general phenomenon in such Hermitian systems.

The critical coupling strength $\Omega_{SSE} = \gamma/\sqrt{2}$ does not coincide with the coupling strength corresponding to the EP ($\Omega_{EP} = \gamma/2$), at which the splitting in the non-Hermitian system (5) appears. However, the coupling strength corresponding to the EP is calculated without taking into account the noise terms. The presence of noise leads to the fact that splitting in the spectrum of the second oscillators occurs at the coupling strength $\Omega = \gamma/\sqrt{2}$ (see Appendix C and Ref. [17]) that coincides with Ω_{SSE} . Therefore, the splitting in the second components $(e_k)_2$ can be associated with the splitting in the spectrum of the stochastic non-Hermitian system.

V. SPONTANEOUS SYMMETRY EMERGENCE

The change in eigenstates manifests itself in the temporal dynamics of the Hermitian system (2)-(4). To illustrate this fact, we calculate the temporal dynamics of the oscillators [Figure 4]. When $\Omega < \Omega_{SSE}$, the absolute value of the amplitude of the first oscillator is smaller than the one of the second oscillator [Figure 4(a)]. It is due to the fact that the first oscillator interacts with the set of oscillators, while the second oscillator does not. With increasing coupling strength, the dynamics of the oscillators' amplitudes become similar to each other [Figures 4(b), (c)]. At the same time, the phase difference between the oscillators changes with time for both $\Omega < \Omega_{SSE}$ and $\Omega > \Omega_{SSE}$ (see [Figure 6] in the Appendix D). Therefore, the transition at $\Omega = \Omega_{SSE}$ is not related to phase locking [57].

To trace out the changes in the oscillators' amplitudes,

we calculate the ratio of the absolute values of the amplitudes of the first and second oscillators averaged over time $\langle \dots \rangle_t$. To begin with, we choose $a_1(t=0) = (\mathbf{e}_+)_1$, $a_2(t=0) = (\mathbf{e}_+)_2$ (see Eq. (6)), and $b_k(t=0) = 0$ as the initial state. When the averaging is carried out over a time interval before the first revival ($0 \leq t < T_R$), the ratio $\langle |a_1| \rangle_t / \langle |a_2| \rangle_t$ demonstrates the threshold-like behavior at $\Omega = \Omega_{EP}$ [Figure 2]. This behavior is similar to the one observed in the non-Hermitian equation (5) at spontaneous symmetry breaking. This similarity in the behaviors of the Hermitian and non-Hermitian systems is due to the fact that at times $t < T_R$, the behavior of $a_1(t)$ and $a_2(t)$ in the Hermitian system can be described approximately by the non-Hermitian Eq. (5). However, at $t > T_R$ the behavior of $a_1(t)$ and $a_2(t)$ in the Hermitian system differs qualitatively from the one in the non-Hermitian system [Figure 4]. When $a_1(t)$ and $a_2(t)$ are averaged over a time interval containing a large number of collapses and revivals ($0 \leq t < t_{\max}$, where $t_{\max} \gg T_R$), the ratio $\langle |a_1| \rangle_t / \langle |a_2| \rangle_t$ demonstrates the threshold-like behavior at $\Omega = \Omega_{SSE}$ [Figure 2]. Thus, it is seen that in the Hermitian system, the symmetry appears at $\Omega = \Omega_{SSE}$. Note that the Eqns. (2)-(4) for the Hermitian system do not possess symmetry with respect to the permutation of the first and second oscillators. That is, the symmetry emerges in the system, which has no such symmetry. Similar behavior takes place for other initial states. To illustrate this fact, we calculate the ratio of the absolute values of the amplitudes of the first and second oscillators averaged over time and then over the initial states, $\langle \langle |a_1| \rangle_t / \langle |a_2| \rangle_t \rangle_0$ [Figure 5]. Our calculations show that when the averaging is carried out over a time interval before the first revival ($0 \leq t < T_R$), the ratio $\langle \langle |a_1| \rangle_t / \langle |a_2| \rangle_t \rangle_0$ increases smoothly with the coupling strength Ω (see [Figure 7] in Appendix D). Instead, when the averaging is carried out over a time interval containing a large number of the collapses and revivals ($0 \leq t < t_{\max}$, where $t_{\max} \gg T_R$), the ratio $\langle \langle |a_1| \rangle_t / \langle |a_2| \rangle_t \rangle_0$ demonstrates the threshold-like behavior at $\Omega = \Omega_{SSE}$ [Figure 5].

VI. DEPENDENCE OF THE SYSTEM BEHAVIOR ON THE NUMBER OF OSCILLATORS IN THE SET

To prove the existence of the transition in the considered system, we study the dependence of $\langle \langle |a_1| \rangle_t / \langle |a_2| \rangle_t \rangle_0$ on the number of oscillators in the set. The frequencies of the oscillators in the set uniformly fill the interval from $-N\delta\omega/2$ to $N\delta\omega/2$. To keep the frequency interval unchanged, we scale $\delta\omega$ as N^{-1} ($N\delta\omega = \text{const}$, i.e., we increase the density of states in the set of the oscillators). The increase in the density of states leads to an enhancement of the energy exchange between the first oscillator and the set of oscillators. Based on the expression for the relaxation rate, $\gamma = \pi g^2 / \delta\omega$, (10), we conclude that such an enhancement is proportional to $1/\delta\omega \sim N$.

To keep the magnitude of the interaction of the first oscillator with the set of oscillators constant, we scale g as $1/\sqrt{N}$ (see Appendix E). Our calculations show that such a scaling preserves the behavior of the eigenstates of the Hermitian system (see [Figure 8] in Appendix E). The change of $\delta\omega$ causes the change in the return time ($T_R = 2\pi/\delta\omega$). To keep the number of revivals and collapses occurring during the observation time, we scale the observation time as N .

Our calculations show that when the averaging of $\langle \langle |a_1| \rangle_t / \langle |a_2| \rangle_t \rangle_0$ is carried out over a time interval containing a large number of collapses and revivals, the increase in N makes the transition at $\Omega = \Omega_{SSE}$ sharper [Figure 5]. In the limit of an infinite set ($\delta\omega/\omega_0 \rightarrow 0$ and $N \rightarrow \infty$), at $\Omega > \Omega_{SSE}$ the ratio $\langle \langle |a_1| \rangle_t / \langle |a_2| \rangle_t \rangle_0$ tends to 1 [Figure 5]. Thus, the oscillators' amplitudes become equal to each other, and in such a sense, the system dynamics become symmetric with respect to the permutation of the oscillators. Note that the system (1) is not symmetric with respect to the permutation of the oscillators. That is, the symmetry spontaneously emerges in the system dynamics, leading to the threshold change in the dependence of $\langle \langle |a_1| \rangle_t / \langle |a_2| \rangle_t \rangle_0$ on the coupling strength [Figure 5]. We name this phenomenon as a spontaneous symmetry emergence. The spontaneous symmetry emergence can be considered as a new class of phase transitions connected with a change in symmetry of the system states.

Note that when the averaging of $\langle \langle |a_1| \rangle_t / \langle |a_2| \rangle_t \rangle_0$ is carried out over the time interval smaller than the time of first revival, the increase of the number of the oscillators in the set ($\delta\omega/\omega_0 \rightarrow 0$ and $N \rightarrow \infty$) does not lead to an appearance of the threshold (see [Figure 7] in Appendix D). Thus, the spontaneous symmetry emergence is observed only when the averaging is carried out over a long time interval ($t \gg T_R$), during which a large number of collapses and revivals take place [Figure 5]. It indicates that the spontaneous symmetry emergence is the property of the entire Hermitian system (1) and cannot be associated with the properties of the non-Hermitian system (5) obtained by the elimination of the degrees of freedom of the set of oscillators.

VII. DISCUSSION

The symmetry with respect to the permutation of the oscillators begins to emerge at the coupling strength $\Omega = \Omega_{SSE}$. It is the coupling strength at which the change in eigenstates occurs. Below the critical coupling, the eigenstates \mathbf{e}_k are not symmetrical with respect to the permutation of the absolute value of the first and second components [Figure 3(a)], and the first and second components of the vast majority of eigenstates differ significantly from each other [Figure 3(a)]. At the critical coupling strength, the peak in the dependence of second components of eigenstates \mathbf{e}_k on their eigenfrequencies f_k splits into two peaks [Figure 3(b)]. At further increases

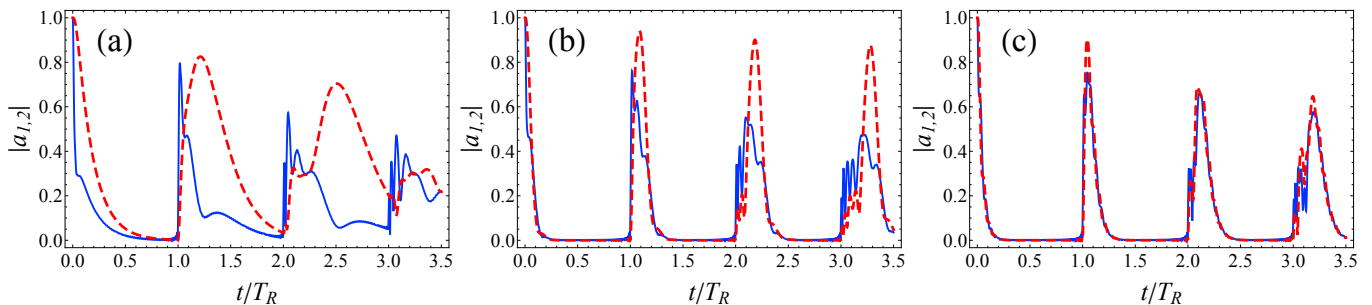


FIG. 4. The dependence of $|a_1(t)|$ (solid blue line) and $|a_2(t)|$ (dashed red line) on time at the coupling strengths $\Omega = 0.5\Omega_{SSE}$ (a), $\Omega = \Omega_{SSE}$ (b), $\Omega = 2\Omega_{SSE}$ (c). Here $T_R = 2\pi/\delta\omega$ is the return time; the number of oscillators in the set is 200. The initial state is $a_1(0) = 1$; $a_2(0) = 1$; $b_k(0) = 0$.

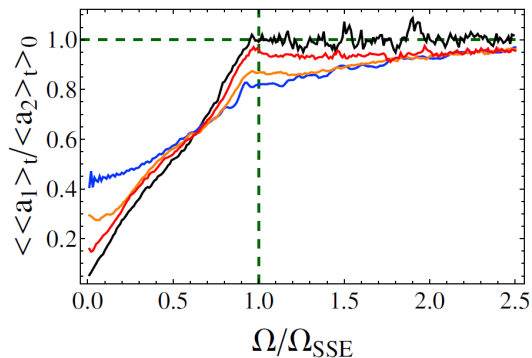


FIG. 5. The dependence of $\langle\langle |a_1| \rangle_t / \langle\langle |a_2| \rangle_t \rangle_0$ on the coupling strength, Ω , when the number of oscillators in the set is $N = 50$ (the blue line), $N = 100$ (the orange line), $N = 200$ (the red line), $N = 400$ (the black line). The dashed vertical line shows the critical coupling strength $\Omega_{SSE} = \gamma/\sqrt{2}$. The dashed horizontal line shows 1. The interval of averaging is $[0, 25 T_R]$. The averaging is carried out over 200 initial states.

in the coupling strength, the eigenstates begin to become symmetrical with respect to the permutation of the first and second components [Figure 3(b), (c), (d)].

The transformation of the eigenstates causes the change in the oscillators' amplitudes. The main contribution to the amplitudes of the first and second oscillators is given by the eigenstates, which have the greatest values of the corresponding components. Therefore, below the critical coupling strength ($\Omega < \Omega_{SSE}$), the main contribution to the amplitude of the second oscillator $\langle\langle |a_2| \rangle_t$ is given by the eigenstates, the eigenfrequencies of which lie within the width of peak at $f_k = \omega_0$ [the red line in Figure 3(a)]. At the same time, the main contribution to the amplitude of the first oscillator $\langle\langle |a_1| \rangle_t$ is given by the eigenstates, the eigenfrequencies of which lie within the widths of two peaks at $f_k \neq \omega_0$ [the blue line in Figure 3(a)]. The numbers of eigenstates, giving the main contribution to $\langle\langle |a_1| \rangle_t$, depend on Ω , while the numbers of eigenstates, giving the main contribution to $\langle\langle |a_2| \rangle_t$, do not. Above the critical coupling strength ($\Omega > \Omega_{SSE}$), the main contributions to the amplitudes of both oscillators come from the eigenstates, the eigenfre-

quencies of which lie within the line widths of two peaks at $f_k \neq \omega_0$ [Figures 3(c), (d)]. Moreover, at $\Omega > \Omega_{SSE}$, the numbers of eigenstates, giving the main contributions to both $\langle\langle |a_1| \rangle_t$ and $\langle\langle |a_2| \rangle_t$, depend on Ω . Thus, the dependence of $\langle\langle |a_2| \rangle_t$ on the coupling strength undergoes qualitative change, which manifests itself in the threshold behavior of $\langle\langle |a_1| \rangle_t / \langle\langle |a_2| \rangle_t$ [Figure 5]. With the increase in coupling strength, the first and second components of eigenstates become similar to each other [Figure 3(d)]. Our analytical estimations show that (see Appendix F) the ratio of $\langle\langle |a_1| \rangle_t / \langle\langle |a_2| \rangle_t$ is determined by the ratio of $P_1\sqrt{\Gamma_1}/P_2\sqrt{\Gamma_2}$, where $P_{1,2} = \max(e_k)_{1,2}^2$ are the heights of peaks, $\Gamma_{1,2}$ are the widths of the peaks (if there are two peaks, then $\Gamma_{1,2}$ are the sum of the widths of both the peaks). This ratio does not depend on the peak frequencies. Above the critical point, the ratio of $P_1\sqrt{\Gamma_1}/P_2\sqrt{\Gamma_2}$ tends to 1 (see Appendix F for details) and, therefore, the ratio of $\langle\langle |a_1| \rangle_t / \langle\langle |a_2| \rangle_t$ tends to 1 too. Thus, the emergence of the symmetry in the system dynamics can be unambiguously associated with the changes in the eigenstates.

VIII. CONCLUSION

We predict the existence of a new class of phase transitions that relate to the emergence of symmetry in the state of the Hermitian system, the Hamiltonian of which does not possess such a symmetry. In other words, the symmetry emerges spontaneously in the system's behavior. This phenomenon is the counterpart of spontaneous symmetry breaking, which is a conventional concomitant of second-order phase transitions. From the point of view of an external observer, spontaneous symmetry emergence has the same manifestations as spontaneous symmetry breaking. Indeed, in both cases, the symmetry of the system state changes at the transition point. However, in contrast to the case of spontaneous symmetry breaking, in which the system Hamiltonian has the same symmetry as the state in symmetrical phase, in the case of spontaneous symmetry emergence, the system Hamiltonian does not have the emerged symmetry.

The spontaneous symmetry emergence is the source of a new class of phase transitions with a change in symmetry; for example, in an optical system consisting of two coupled single-mode cavities, one of which interacts with a waveguide of finite length. Thus, our results open the way to the study of phase transitions with the change of the symmetry in Hermitian systems without symmetry.

ACKNOWLEDGEMENT

The study was financially supported by a Grant from Russian Science Foundation (Project No. 20-72-10057). T.T.S. thanks foundation for the advancement of theoretical physics and mathematics ‘‘Basis’’.

APPENDIX A. DERIVATION OF THE SYSTEMS’ EQUATIONS

We consider the system of two coupled oscillators, one of which interacts with a finite set of oscillators. The Hamiltonian of the system is

$$\hat{H} = \omega_0 \hat{a}_1^\dagger \hat{a}_1 + \omega_0 \hat{a}_2^\dagger \hat{a}_2 + \Omega \left(\hat{a}_1^\dagger \hat{a}_2 + \hat{a}_2^\dagger \hat{a}_1 \right) + \sum_{k=1}^N \omega_k \hat{b}_k^\dagger \hat{b}_k + \sum_{k=1}^N g \left(\hat{b}_k^\dagger \hat{a}_1 + \hat{a}_1^\dagger \hat{b}_k \right) \quad (8)$$

where $\hat{a}_{1,2}$ and $\hat{a}_{1,2}^\dagger$ are the annihilation and creation operators of the first and second oscillators, $[\hat{a}_j, \hat{a}_k^\dagger] = \delta_{jk}$ [5]. \hat{b}_k and \hat{b}_k^\dagger are the annihilation and creation operators of the oscillators in the set with the frequencies $\omega_k = \omega_0 + \delta\omega \left(k - \frac{N}{2} \right)$, $[\hat{b}_j, \hat{b}_k^\dagger] = \delta_{jk}$. Ω is a coupling strength between the first and second oscillators. g is a coupling strength between the first oscillator and each of the oscillators in the set. For convenience, we consider that $\hbar = 1$. Using the Heisenberg equation for operators $\frac{d\hat{A}}{dt} = i [\hat{H}, \hat{A}]$ [5], we obtain the following equations:

$$\begin{aligned} \frac{d\hat{a}_1}{dt} &= i [\hat{H}, \hat{a}_1] = -i\omega_0 \hat{a}_1 - i\Omega \hat{a}_2 - i \sum_{k=1}^N g \hat{b}_k \\ \frac{d\hat{a}_2}{dt} &= i [\hat{H}, \hat{a}_2] = -i\omega_0 \hat{a}_2 - i\Omega \hat{a}_1 \\ \frac{d\hat{b}_k}{dt} &= i [\hat{H}, \hat{b}_k] = -i\omega_k \hat{b}_k - ig \hat{a}_1 \end{aligned} \quad (9)$$

One can notice that the system (9) is linear and then we can move from equations for operators to closed system of equations for their averages:

$$\frac{da_1}{dt} = -i\omega_0 a_1 - i\Omega a_2 - i \sum_{k=1}^N g b_k \quad (10)$$

$$\frac{da_2}{dt} = -i\omega_0 a_2 - i\Omega a_1 \quad (11)$$

$$\frac{db_k}{dt} = -i\omega_k b_k - ig a_1 \quad (12)$$

Here we use the notations $\langle \hat{a}_1 \rangle = a_1$, $\langle \hat{a}_2 \rangle = a_2$ and $\langle \hat{b}_k \rangle = b_k$. Note that since the operators’ equations do not contain the products of the operators (e.g. $\hat{a}_1 \hat{a}_2$) then the transition to the operators’ averages is exact.

APPENDIX B. DERIVATION OF THE EQUATIONS FOR NON-HERMITIAN SYSTEM

The transition to a non-Hermitian system can be carried out by increasing the number of modes in the reservoir to infinity with simultaneous decreasing the distance between the neighboring modes to zero ($N \rightarrow \infty$ and $\delta\omega/\omega_0 \rightarrow 0$). In this limit, the characteristic time of the revival of the oscillations ($T_R = \frac{2\pi}{\delta\omega}$) [55] is much longer than the observation time. Therefore, the system dynamics are described only by the exponential decay stage, as it takes place in the non-Hermitian system.

To derive the non-Hermitian equations describing the system dynamics during the exponential stage, we first formally integrate the equation (12)

$$b_k = b_k(0) e^{-i\omega_k t} - ig \int_0^t d\tau a_1(\tau) e^{-i\omega_k(t-\tau)} \quad (13)$$

After substituting the Eq. (13) into the Eq. (10), we obtain

$$\dot{a}_1 = -i\omega_0 a_1 - i\Omega a_2 - \sum_k g^2 \int_0^t d\tau a_1(\tau) e^{-i\omega_k(t-\tau)} \quad (14)$$

Here we assume that $b_k(0) = 0$. Note that such initial state we use in all our calculations.

Using the Born-Markovian approximation [45, 46] and Sokhotskii-Plemelj formula [58], one can calculate the integral in the equation (14) and obtain the following equations for non-Hermitian system [45, 59]:

$$\begin{aligned} \dot{a}_1 &= (-i\omega_0 - \gamma) a_1 - i\Omega a_2 \\ \dot{a}_2 &= -i\omega_0 a_2 - i\Omega a_1 \end{aligned} \quad (15)$$

Here the decay rate γ in (15) is determined by the following formula [45]

$$\gamma = \sum_k \pi g^2 \delta(\omega_k - \omega_0) \quad (16)$$

where $\delta(\omega)$ is Dirac’s delta-function.

The formula 16 can be simplified by substituting $\omega_k = \omega_0 + \delta\omega \left(k - N/2 \right)$. Then we obtain

$$\gamma = \frac{\pi g^2}{\delta\omega} \quad (17)$$

APPENDIX C. NON-HERMITIAN EQUATIONS WITH NOISE

In Appendix B, we used the assumption that $b_k(0) = 0$, so we excluded the thermal effects of the environment on the system from consideration. However, in order to consider the radiation of such a system, it is necessary to take into account the noise in the system. Now, we assume that $b_k(0) \neq 0$. Then equations (15) will take the form of equations with noise (5):

$$\frac{d}{dt} \begin{pmatrix} a_1 \\ a_2 \end{pmatrix} = \begin{pmatrix} -i\omega_0 - \gamma & -i\Omega \\ -i\Omega & -i\omega_0 \end{pmatrix} \begin{pmatrix} a_1 \\ a_2 \end{pmatrix} + \begin{pmatrix} \xi \\ 0 \end{pmatrix} \quad (18)$$

where $\xi(t) = -i \sum_k g b_k(0) e^{-i(\omega_k - \omega_0)t}$, according to fluctuation-dissipation theorem [41, 45, 46], is the noise

term with the following correlations:

$$\langle \xi(t) \rangle = 0 \quad (19)$$

$$\langle \xi^*(t + \tau) \xi(t) \rangle = \gamma T \delta(\tau) \quad (20)$$

where γ is determined by Eq. (17) and T is the temperature of the environment. In this model it is possible to calculate the spectrum of the two main oscillators (see Eq. (6) in Ref. [17]). Then we can calculate the value of coupling strength, Ω_2^{split} , when the splitting of the second oscillator's spectrum appears. To do this, we can use the formula from our work [17] that was obtained for more general models in which each oscillator interacts with its reservoir (see pp. 9 - 10 in Ref. [17]):

$$(\Omega_2^{split})^2 = \frac{\gamma_2^2 \gamma_1 T_1 + \gamma_1^3 T_1 - 2\gamma_1^2 \gamma_2 T_2 - 2\gamma_2^2 \gamma_1 T_2}{2(\gamma_2 T_2 + 2\gamma_1 T_1)} + \frac{\sqrt{4\gamma_2 \gamma_1^4 T_2 (\gamma_2 T_2 + 2\gamma_1 T_1) + (\gamma_1 (\gamma_1^2 + \gamma_2^2) T_1 - 2\gamma_1 \gamma_2 (\gamma_1 + \gamma_2) T_2)^2}}{2(\gamma_2 T_2 + 2\gamma_1 T_1)} \quad (21)$$

Here γ_1, γ_2 are the relaxation rates of the first and second oscillators. T_1 and T_2 are temperatures of the reservoirs interacting with the first and second oscillators, respectively.

Using the fact that the our system has only one reservoir, i.e. $\gamma_1 = \gamma, \gamma_2 = 0, T_1 = T$ and $T_2 = 0$, we finally obtain:

$$\Omega_2^{split} = \gamma / \sqrt{2} \quad (22)$$

This value of coupling strength determines the critical coupling strength, above which the splitting of the eigenstates of the Hermitian system occurs [see red lines in Figure 3], i.e. $\Omega_2^{split} = \Omega_{SSE} = \gamma / \sqrt{2}$. Note that the spectrum of the first oscillator is always splitted, which is also predicted by the considered model [see blue lines in Figure 3].

APPENDIX D. DYNAMICS OF THE HERMITIAN SYSTEM AT DIFFERENT COUPLING STRENGTH BETWEEN THE OSCILLATORS

We use the Eqns. (10)–(12) to describe the dynamics of the Hermitian system (8). We calculate the temporal evolution of the oscillators' amplitudes, $|a_{1,2}(t)|$, and the phase difference between the oscillators, $\Delta\phi(t) = \arg(a_1(t)) - \arg(a_2(t))$ [Figure 6]. When the coupling strength between the oscillators $\Omega \ll \Omega_{SSE}$, the temporal dynamics of $|a_1(t)|$ and $|a_2(t)|$ are very different from each other [Figure 6(a)]. Increasing the coupling strength causes the temporal dynamics of $|a_1(t)|$ and $|a_2(t)|$ to become more similar [Figure 6(c) and (e)]. In turn, when

$\Omega \ll \Omega_{SSE}$, the phase difference between the oscillators, $\Delta\phi(t)$, changes noticeably during the collapses and revivals [Figure 6(b)]. In the time intervals between revivals, the phase difference, $\Delta\phi(t)$, changes slightly, but still is not constant in time [Figure 6(b)]. The increase in the coupling constant leads to the phase difference begins to change noticeably at all times [Figure 6(d) and (f)]. Thus, we can conclude that the phase transition occurring at $\Omega = \Omega_{SSE}$ (see the main text) is not related to the phase locking of the oscillators [57].

The changes in the system dynamics during the increase of Ω clearly manifest in the dependence of $\langle\langle |a_1| \rangle_t / \langle\langle |a_2| \rangle_t \rangle_0$ on the coupling strength Ω , where $\langle\langle |a_{1,2}| \rangle_t = \frac{1}{t_{\max}} \int_0^{t_{\max}} |a_{1,2}(t)| dt$ and $\langle\langle \dots \rangle_0$ denotes averaging over initial conditions. Our calculation shows that when the averaging of $\langle\langle |a_1| \rangle_t / \langle\langle |a_2| \rangle_t \rangle_0$ is carried out over time interval containing large number of the collapses and revivals, the dependence of $\langle\langle |a_1| \rangle_t / \langle\langle |a_2| \rangle_t \rangle_0$ on the coupling strength demonstrates a clear threshold at $\Omega = \Omega_{SSE}$ [Figure 5 in the main text]. The increase of the number of oscillators in the set ($N \rightarrow \infty$ and $\delta\omega/\omega_0 \rightarrow 0$) makes the transition at $\Omega = \Omega_{SSE}$ sharper [Figure 7(a) and Figure 5 in the main text]. At the same time, when the averaging of $\langle\langle |a_1| \rangle_t / \langle\langle |a_2| \rangle_t \rangle_0$ is carried out over a time interval smaller than the time of first revival, the dependence of $\langle\langle |a_1| \rangle_t / \langle\langle |a_2| \rangle_t \rangle_0$ on the coupling strength is smooth [Figure 7(b)]. In this case, the increase in N ($N \rightarrow \infty$ and $\delta\omega/\omega_0 \rightarrow 0$) does not lead to the appearance of a sharp threshold [Figure 7]. This confirms that the predicted transition is due to the Hermitian dynamics of the system at times much longer than the return time.

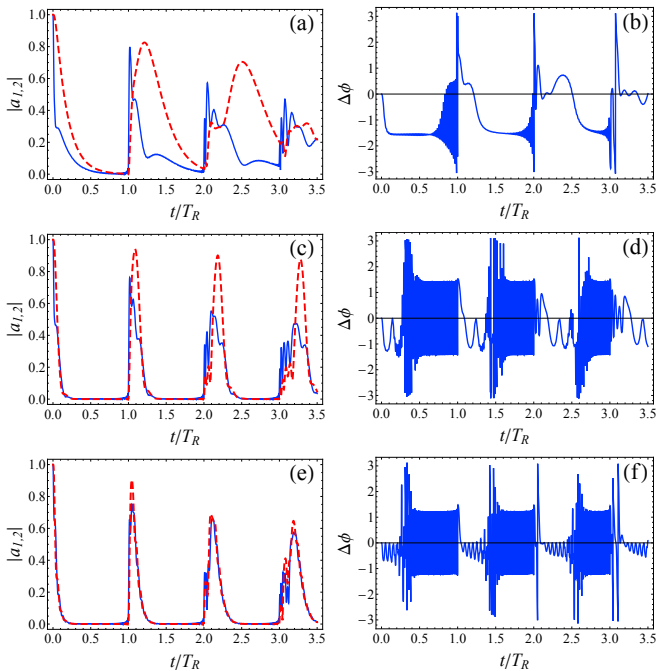


FIG. 6. (a), (c), (e) The dependence of $|a_1(t)|$ (solid blue line) and $|a_2(t)|$ (dashed red line) on time. (b), (d), (f) The dependence of the phase difference between the amplitudes of the first and second oscillators ($\Delta\phi = \arg(a_1(t)) - \arg(a_2(t))$) on time. The coupling strength between the oscillators is $\Omega = 0.5\Omega_{SSE}$ (a), (b); $\Omega = \Omega_{SSE}$ (c), (d); $\Omega = 2\Omega_{SSE}$ (e), (f). Here $T_R = 2\pi/\delta\omega$ is a return time; the number of oscillators in the set is 200. The initial state is $a_1(0) = 1$; $a_2(0) = 1$; $b_k(0) = 0$.

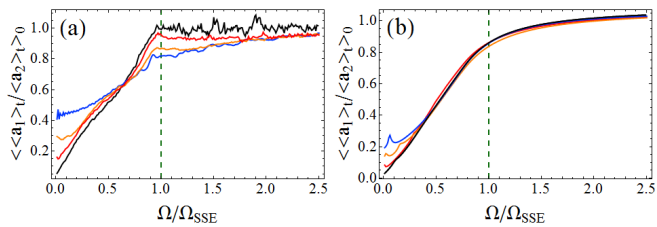


FIG. 7. The dependence of $\langle\langle |a_1| \rangle_t / \langle\langle |a_2| \rangle_t \rangle_0$ on the coupling strength Ω when the number of oscillators in the set $N = 50$ (the blue line), $N = 100$ (the orange line), $N = 200$ (the red line), $N = 400$ (the black line). The interval of averaging is $[0, 25T_R]$ (a) and $[0, 0.5T_R]$ (b). The dashed vertical line shows the critical coupling strength $\Omega_{SSE} = \gamma/\sqrt{2}$, where $\gamma = \pi g^2/\delta\omega$. The averaging is carried out over 200 initial states. When the number of the oscillators (N) change, g is scaled as $1/\sqrt{N}$ and $\delta\omega$ is scaled as $1/N$.

APPENDIX E. SCALING THE SYSTEM PARAMETERS

We study the dependence of $\langle\langle |a_1| \rangle_t / \langle\langle |a_2| \rangle_t \rangle_0$ on the number of oscillators in the set, N . The frequencies of the oscillators in the set uniformly fill the interval from $\omega_0 - N\delta\omega/2$ to $\omega_0 + N\delta\omega/2$. To keep the frequency interval

unchanged, we scale $\delta\omega$ as N^{-1} ($N\delta\omega = const$, i.e. the density of states in the reservoir increases). The increase in N leads to the enhancement of the energy exchange between the first oscillator and the set of oscillators. Based on the expression for the relaxation rate, γ , (10), we conclude that such an enhancement is proportional to $1/\delta\omega \sim N$. To keep the magnitude of the relaxation rate, we scale g (coupling strength between the first oscillator and each of the oscillators in the set) as $N^{-1/2}$.

Our numerical simulation shows that the increase in the number of oscillators in the set ($N \rightarrow \infty$, $\delta\omega \sim N^{-1}$, $g \sim N^{-1/2}$) makes the transition at $\Omega = \Omega_{SSE}$ sharper [Figure 5 in the main text]. To prove that the phase transition appears due to the change in the eigenstates [Figure 3 in the main text], we calculate the eigenstates for different N . Our calculations show that at the parameter scaling described above ($\delta\omega \sim N^{-1}$, $g \sim N^{-1/2}$), an increase in N preserves the behavior of the eigenstates (Figure 8). At $\Omega < \Omega_{SSE}$, the value of the second component of the eigenstate with eigenfrequency $f_k = \omega_0$ is larger than the value of the second component of any other eigenstate [see the first line in Figure 8]. In contrast, this eigenstate with $f_k = \omega_0$ has a zero value of the first component [see the first line in Figure 8]. The increase in the coupling strength leads to a splitting of the peak in the dependence of the second components of the eigenstates on their eigenfrequencies. This splitting begins to appear at the critical coupling strength $\Omega = \Omega_{SSE}$ [the second line in Figure 8]. At $\Omega > \Omega_{SSE}$, both components of the eigenstates have two peaks [the third and fourth lines in Figure 8]. Thus, we conclude that the increase in N does not change the value of Ω at which the splitting in the eigenstates occurs.

APPENDIX F. EMERGENCE OF SYMMETRY FOR NON-SYMMETRICAL EIGENSTATES

The eigenstates experience the qualitative change at the coupling strength $\Omega = \Omega_{SSE}$. When Ω increases above Ω_{SSE} , the amplitudes of first ($(e_k)_1$ (blue points) and second ($(e_k)_2$ (red points) components in the eigenstate \mathbf{e}_k become more symmetrical [Figure 8]. This symmetrization occurs smoothly. At the same time, the ratio $\langle\langle |a_1| \rangle_t / \langle\langle |a_2| \rangle_t \rangle_0$ demonstrates the threshold behavior on the coupling strength $\Omega = \Omega_{SSE}$.

To comprehend the source of the sharp symmetrization of $\langle\langle |a_1| \rangle_t / \langle\langle |a_2| \rangle_t \rangle_0$ at $\Omega = \Omega_{SSE}$, we consider in more details the system dynamics. The dynamics of the first and second oscillators can be described by the following formula:

$$a_{1,2}(t) = \sum_{k=1}^{N+2} C_k(e_k)_{1,2} e^{i f_k t} \quad (23)$$

where f_k are the eigenfrequencies of the Eqns. (10)-(12), $(e_k)_{1,2}$ are the first and second components of the

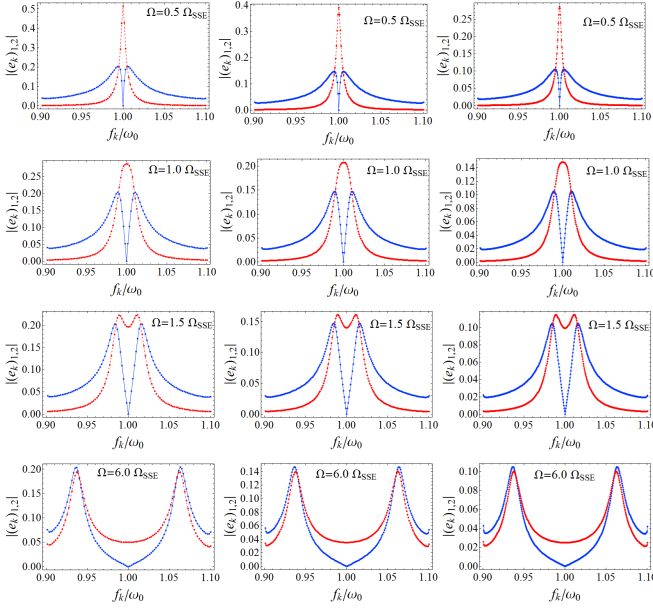


FIG. 8. The dependence of the amplitudes of first $(e_k)_1$ (blue points) and second $(e_k)_2$ (red points) components in the eigenstate \mathbf{e}_k on its eigenfrequency f_k for the different coupling strengths: $\Omega = 0.5 \Omega_{SSE}$ (first row); $\Omega = \Omega_{SSE}$ (second row); $\Omega = 1.5 \Omega_{SSE}$ (third row); $\Omega = 6 \Omega_{SSE}$ (fourth row). Here $\Omega_{SSE} = \gamma/\sqrt{2}$ and $\gamma = \pi g^2/\delta\omega$. The left column is plotted for 100 oscillators in the set; the center column is plotted for 200 oscillators in the set; and the right column is plotted for 400 oscillators in the set. When the number of the oscillators N changes, g is scaled as $1/\sqrt{N}$ and $\delta\omega$ is scaled as $1/N$.

eigenstates and C_k are the decomposition coefficients of initial conditions by eigenstates, which are given as $C_k = a_1^{(0)}(e_k)_1^* + a_2^{(0)}(e_k)_2^*$, where $a_1^{(0)}$ and $a_2^{(0)}$ are initial amplitudes of the first and second oscillators, respectively. N is a number of the oscillators in the set.

It is important that all $(e_k)_{1,2}$ can be chosen to be real at the same time. Then the temporal dependences for the amplitudes of first and second oscillators are given as

$$a_1(t) = a_1^{(0)} \sum_{k=1}^{N+2} (e_k)_1^2 e^{i f_k t} + a_2^{(0)} \sum_{k=1}^{N+2} (e_k)_1 (e_k)_2 e^{i f_k t} \quad (24)$$

$$a_2(t) = a_2^{(0)} \sum_{k=1}^{N+2} (e_k)_2^2 e^{i f_k t} + a_1^{(0)} \sum_{k=1}^{N+2} (e_k)_1 (e_k)_2 e^{i f_k t} \quad (25)$$

We introduce a notation $\xi(t) = \sum_{k=1}^{N+2} (e_k)_1 (e_k)_2 e^{i(f_k - \omega_0)t}$ and find the expressions for the absolute values of the

oscillators amplitudes

$$|a_1(t)| = \left(|a_1^{(0)}|^2 \left| \sum_{k=1}^{N+2} (e_k)_1^2 e^{i f_k t} \right|^2 + |a_2^{(0)}|^2 |\xi(t)|^2 + 2 \operatorname{Re} \left(a_1^{(0)} a_2^{(0)*} \sum_{k=1}^{N+2} (e_k)_1^2 e^{i f_k t} \xi^*(t) \right) \right)^{1/2} \quad (26)$$

$$|a_2(t)| = \left(|a_2^{(0)}|^2 \left| \sum_{k=1}^{N+2} (e_k)_2^2 e^{i f_k t} \right|^2 + |a_1^{(0)}|^2 |\xi(t)|^2 + 2 \operatorname{Re} \left(a_2^{(0)} a_1^{(0)*} \sum_{k=1}^{N+2} (e_k)_2^2 e^{i f_k t} \xi^*(t) \right) \right)^{1/2} \quad (27)$$

The last terms in the Eqns. (26) and (27) are sign-alternating and, when averaging over time, their contributions tend to zero [Figure 9]. Therefore, the following equation takes place

$$\frac{\langle |a_1| \rangle_t}{\langle |a_2| \rangle_t} \approx \frac{\int_0^T \sqrt{|a_1^{(0)}|^2 \left| \sum_{k=1}^{N+2} (e_k)_1^2 e^{i f_k t} \right|^2 + |a_2^{(0)}|^2 |\xi(t)|^2} dt}{\int_0^T \sqrt{|a_2^{(0)}|^2 \left| \sum_{k=1}^{N+2} (e_k)_2^2 e^{i f_k t} \right|^2 + |a_1^{(0)}|^2 |\xi(t)|^2} dt} \quad (28)$$

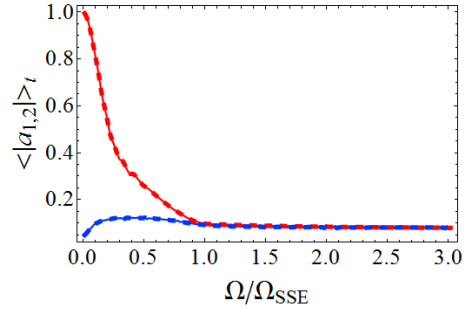


FIG. 9. The dependences of the amplitudes of the first (blue lines) and second (red lines) oscillators averaged over time on the coupling strength between the oscillators. The solid lines calculated with taking into account the sign-alternating terms in the Eqns. (26), (27); the dashed lines calculated without taking into account the sign-alternating terms.

When averaging over the initial states, the factors $|a_1^{(0)}|^2$ and $|a_2^{(0)}|^2$ are equal to each other. In this case, the ratio

$$\langle |a_1| \rangle_t / \langle |a_2| \rangle_t \approx \frac{\int_0^T \sqrt{\left| \sum_{k=1}^{N+2} (e_k)_1^2 e^{i f_k t} \right|^2 + |\xi(t)|^2} dt}{\int_0^T \sqrt{\left| \sum_{k=1}^{N+2} (e_k)_2^2 e^{i f_k t} \right|^2 + |\xi(t)|^2} dt} \quad (29)$$

demonstrates a clear transition at $\Omega = \Omega_{SSE}$ [Figure 10(a)]. The second terms in the ratio are the same, therefore, this ratio is determined by the relation between

$$\left| \sum_{k=1}^{N+2} (e_k)_1^2 e^{i f_k t} \right|^2 \text{ and } \left| \sum_{k=1}^{N+2} (e_k)_2^2 e^{i f_k t} \right|^2.$$

Our calculations show that the ratio (28) without the second terms, i.e., $\int_0^T \left| \sum_{k=1}^{N+2} (e_k)_1^2 e^{i f_k t} \right| dt / \int_0^T \left| \sum_{k=1}^{N+2} (e_k)_2^2 e^{i f_k t} \right| dt$, also demonstrates a clear transition at $\Omega = \Omega_{SSE}$ [Figure 10(b)]. Thus, we can assume that the transition is due to the changes in the expressions $\int_0^T \left| \sum_{k=1}^{N+2} (e_k)_{1,2}^2 e^{i f_k t} \right| dt$. These expressions can be rewritten as

$$\int_0^T \left| \sum_{k=1}^{N+2} (e_k)_{1,2}^2 e^{i f_k t} \right| dt = \int_0^T \left(\sum_{k=1}^{N+2} (e_k)_{1,2}^4 + \sum_{k=1}^{N+2} \sum_{m=1}^{N+2} (e_k)_{1,2}^2 (e_m)_{1,2}^2 e^{i(f_k - f_m)t} \right)^{1/2} dt \quad (30)$$

where, in the double sum, $k \neq m$.

The first term in the Eq. (30) does not depend on time, whereas the second term oscillates in time in a complex way. The presence of the oscillating term is necessary for existence of the transition in the considered system. Indeed, our calculation shows that the ratio

$$\int_0^T \sqrt{\sum_{k=1}^{N+2} (e_k)_1^4} dt / \int_0^T \sqrt{\sum_{k=1}^{N+2} (e_k)_2^4} dt$$

does not demonstrate the threshold behavior and smoothly tends to 1 when the coupling strength increases [Figure 10(c)]. Thus, the interference between the modes plays a key role in the formation of the transition. Note that the total sum

$$\sum_{k=1}^{N+2} \sum_{m=1}^{N+2} (e_k)_{1,2}^2 (e_m)_{1,2}^2 = \sum_{k=1}^{N+2} (e_k)_{1,2}^2 \sum_{m=1}^{N+2} (e_m)_{1,2}^2$$

is equal to 1 ($\sum_{m=1}^{N+2} (e_m)_{1,2}^2 = 1$). For this reason, the transition

manifests itself only at time much greater than the return time, when the phase difference between the various modes becomes significant [cf. Figure 7]. To ascertain the mechanism of the transition appearance, we determine

the main contribution in the sums $\left| \sum_{k=1}^{N+2} (e_k)_{1,2}^2 e^{i f_k t} \right|$. Below

the transition point, the second component $(e_k)_2$ has one peak, whereas, the first component $(e_k)_1$ has two peaks [the first row in Figure 8]. Above the transition point, both components have two peaks. In the case, when the second component has one peak, we can rewrite the expression (30) in the following form

$$\left| \sum_{k=1}^{N+2} (e_k)_2^2 e^{i f_k t} \right| = \left| e^{i \omega_0 t} \sum_{k=1}^{N+2} (e_k)_2^2 e^{i(f_k - \omega_0)t} \right| = \left| \sum_{k=1}^{N+2} (e_k)_2^2 e^{i(f_k - \omega_0)t} \right| \quad (31)$$

where ω_0 is the peak frequency (it coincides with the oscillators frequency).

In the case when the component has two peaks, the expression (30) can be rewritten in the following form

$$\left| \sum_{k=1}^{N+2} (e_k)_{1,2}^2 e^{i f_k t} \right| = \left| e^{i(\omega_0 - \Delta\omega_{1,2})t} \sum_{k=1}^{N/2+1} (e_k)_{1,2}^2 e^{i(f_k - \omega_0 + \Delta\omega_{1,2})t} + e^{i(\omega_0 + \Delta\omega_{1,2})t} \sum_{k=N/2+2}^{N+2} (e_k)_{1,2}^2 e^{i(f_k - \omega_0 - \Delta\omega_{1,2})t} \right| = \left| e^{-i\Delta\omega_{\max}t} \sum_{k=1}^{N/2+1} (e_k)_{1,2}^2 e^{i(f_k - \omega_0 + \Delta\omega_{1,2})t} + e^{i\Delta\omega_{\max}t} \sum_{k=N/2+2}^{N+2} (e_k)_{1,2}^2 e^{i(f_k - \omega_0 - \Delta\omega_{1,2})t} \right| \quad (32)$$

On the right part of the Eq. (32) the first sum includes only the eigenstates with the eigenfrequencies $f_k < \omega_0$ and the second sum includes only the eigenstates with the eigenfrequencies $f_k > \omega_0$. $\omega_0 \pm \Delta\omega_{1,2}$ are the frequencies of peaks for the corresponding components [Figure 8]. Taking into account the dependences of $(e_k)_{1,2}$ on f_k , we conclude that

$$\sum_{k=1}^{N/2+1} (e_k)_{1,2}^2 e^{i(f_k - \omega_0 + \Delta\omega_{\max})t} = (-1)^{1,2} \left(\sum_{k=N/2+2}^{N+2} (e_k)_{1,2}^2 e^{i(f_k - \omega_0 - \Delta\omega_{\max})t} \right)^* \quad (33)$$

Here $(-1)^{1,2}$ denotes that for the first component the sign is a minus and for the second component the sign is a plus.

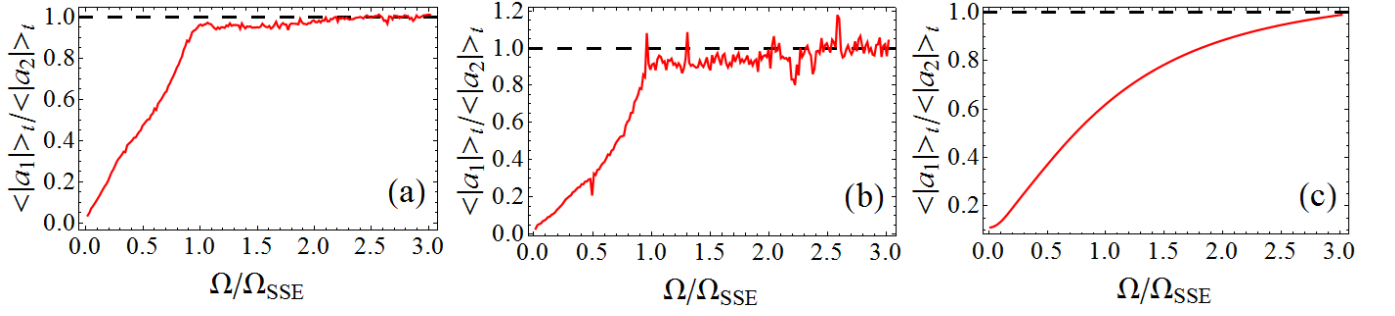


FIG. 10. (a) The dependence of the ratio $\langle |a_1| \rangle_t / \langle |a_2| \rangle_t$ calculated without taking into account the sign-alternating terms in the Eqns. (26), (27), but with taking into account the term $|\xi(t)|^2$, on the coupling strength between the oscillators [Eq. (28)]. The number of the oscillators in the set is 200. (b) The dependence of the ratio $\langle |a_1| \rangle_t / \langle |a_2| \rangle_t$ calculated without taking into account the sign-alternating terms and without taking into account the term $|\xi(t)|^2$ on the coupling strength, i.e. $\int_0^T \left| \sum_{k=1}^{N+2} (e_k)_1^2 e^{i f_k t} \right| dt / \int_0^T \left| \sum_{k=1}^{N+2} (e_k)_2^2 e^{i f_k t} \right| dt$. (c) The dependence of the ratio $\int_0^T \sqrt{\sum_{k=1}^{N+2} (e_k)_1^4} dt / \int_0^T \sqrt{\sum_{k=1}^{N+2} (e_k)_2^4} dt$ on the coupling strength.

Then, we make the following transformation

$$\begin{aligned} & \left| \sum_{k=1}^{N+2} (e_k)_{1,2}^2 e^{i f_k t} \right| = \\ & \left| e^{-i \Delta \omega_{\max} t} \sum_{k=1}^{N/2+1} (e_k)_{1,2}^2 e^{i (f_k - \omega_0 + \Delta \omega_{1,2}) t} + \right. \\ & \left. (-1)^{1,2} e^{i \Delta \omega_{1,2} t} \left(\sum_{k=1}^{N/2+1} (e_k)_{1,2}^2 e^{i (f_k - \omega_0 + \Delta \omega_{1,2}) t} \right)^* \right| = \\ & 2 \left(\left| \sum_{k=1}^{N/2+1} (e_k)_{1,2}^2 e^{i (f_k - \omega_0 + \Delta \omega_{1,2}) t} \right|^2 + (\pm 1)^{1,2} \times \right. \\ & \left. \operatorname{Re} \left(e^{-2i \Delta \omega_{1,2} t} \left(\sum_{k=1}^{N/2+1} (e_k)_{1,2}^2 e^{i (f_k - \omega_0 + \Delta \omega_{1,2}) t} \right)^2 \right) \right)^{1/2} \end{aligned} \quad (34)$$

The second term in the Eq. (34) is sign-alternating and, when averaging over time, their contribution tends to zero. Thus, we obtain the following expressions for the component, which has two peaks

$$\left| \sum_{k=1}^{N+2} (e_k)_{1,2}^2 e^{i f_k t} \right| \approx \sqrt{2} \left| \sum_{k=1}^{N/2+1} (e_k)_{1,2}^2 e^{i (f_k - \omega_0 + \Delta \omega_{1,2}) t} \right| \quad (35)$$

When $t \gg T_R$, due to the eigenfrequencies f_k are not equidistant precisely, the various eigenstates are added to each other with arbitrary phases. The maximal contributions in the sums (31) and (35) are given by the eigenstates with the greatest values of $(e_k)_{1,2}^2$, i.e., the eigenstates, the eigenfrequencies of which lie at the peaks.

It is important that in the case when the eigenstates are added to each other with arbitrary phases ($t \gg T_R$),

the sums (31) and (35) do not depend on the peak frequencies and depend only on the peak form. In the simplest consideration, the peaks are characterized only by the height, $P_{1,2} = \max (e_k)_{1,2}^2$, and widths, $\Gamma_{1,2}$. Within this approximation, the sums (31) and (35) are only functions of $P_{1,2}$ and $\Gamma_{1,2}$. It is clear that the sums (31) and (35) are linearly proportional to $P_{1,2} = \max (e_k)_{1,2}^2$. At the same time, since the various eigenstates are added to each other with arbitrary phases, then the sums (31) and (35) are proportional to the square root of number of the eigenstates within the peak [60]. This number is proportional to the peak widths and, therefore, the sums (31) and (35) are proportional to $\sqrt{\Gamma_{1,2}}$.

Below the transition point, the second component has one peak and the first component has two peaks, and, therefore,

$$\left| \sum_{k=1}^{N+2} (e_k)_2^2 e^{i f_k t} \right| \approx \eta(P_2, \Gamma_2) \sim \sqrt{\Gamma_2} P_2 \quad (36)$$

$$\left| \sum_{k=1}^{N+2} (e_k)_1^2 e^{i f_k t} \right| \approx \sqrt{2} \eta(P_1, \Gamma_1) \sim \sqrt{2 \Gamma_1} P_1 \quad (37)$$

Above the transition point

$$\left| \sum_{k=1}^{N+2} (e_k)_2^2 e^{i f_k t} \right| \approx \sqrt{2} \eta(P_2, \Gamma_2) \sim \sqrt{2 \Gamma_2} P_2 \quad (38)$$

$$\left| \sum_{k=1}^{N+2} (e_k)_1^2 e^{i f_k t} \right| \approx \sqrt{2} \eta(P_1, \Gamma_1) \sim \sqrt{2 \Gamma_1} P_1 \quad (39)$$

It can be seen that when the component has two peaks, the expression (37) is proportional to the square root of total width of the two peaks. Therefore, to estimate

the sum (35) at the transition point, at which the one peak splits into the two peaks, we use the expression (36) considering that Γ_2 is a total width of the split peak and begin to use the expression (38), when the height of minimum between the two peaks becomes less than the half of absolute height.

Using the Eqns. (36)–(39), we calculate the dependences of the sums (31), (35) on the coupling strength. It is important that the expressions (36)–(39) do not depend on time and, therefore, the averaging over time does not change the answer.

Our calculations show that when the coupling strength $\Omega > \Omega_{SSE}$, $\left| \sum_{k=1}^N (e_k)_1^2 e^{i f_k t} \right|$ (the blue line) and $\left| \sum_{k=1}^N (e_k)_2^2 e^{i f_k t} \right|$ (the red line) calculated by the Eqns. (36)–(39) are almost exactly equal to each other [Figure 11(a)]. At the same time, $P_1 \neq P_2$ and $\Gamma_1 \neq \Gamma_2$ almost for all values of the coupling strength [Figure 11(b), (c)], and the first and second components of the eigenstates differ from each other. Thus, the sums $\left| \sum_{k=1}^N (e_k)_{1,2}^2 e^{i f_k t} \right|$ for the first and second components becomes the same, whereas, the first and second components are not the same.

When the eigenstates are added to each other with arbitrary phases, the sums (31) and (35) can be treated as random variables. The ratio of the variance of such a random variable to the averaged value decreases as $1/\sqrt{N}$. For this reason, the increase in the number of oscillators in the set, N , leads to a decrease in the relative fluctuations of each of the sums and the ratio of these sums becomes more exactly equal to 1. Moreover, it can be seen from Figure 8 that an increase in the number of os-

illators, N , leads only to an increase in the density of the eigenstates. Therefore, in the limit of a large number of oscillators, N , a set of eigenstates can be described by a continuous function to which the set converges. In this limit, the approximations (36)–(39) become more accurate, and the ratio of the sums (31) and (35) tends to 1.

The dependence of $\langle |a_1| \rangle_t / \langle |a_2| \rangle_t$ is determined by the ratio of $\left| \sum_{k=1}^N (e_k)_1^2 e^{i f_k t} \right| / \left| \sum_{k=1}^N (e_k)_2^2 e^{i f_k t} \right|$ [Eq. (28)]. Therefore, when $\left| \sum_{k=1}^N (e_k)_1^2 e^{i f_k t} \right| / \left| \sum_{k=1}^N (e_k)_2^2 e^{i f_k t} \right|$ tends to 1, the ratio of $\langle |a_1| \rangle_t / \langle |a_2| \rangle_t$ also comes to 1 [Figure 7(a)].

Thus, the dependence of $\langle |a_1| \rangle_t / \langle |a_2| \rangle_t$ on the coupling strength demonstrates a clear threshold at $\Omega = \Omega_{SSE}$ [see Figure 7(a)] and the system dynamics becomes symmetrical with respect to this characteristic, although the first and second components of the eigenstates are not symmetrical [Figure 8]. This is due to the fact that when $t \gg T_R$, the averages $\langle |a_1| \rangle_t$ and $\langle |a_2| \rangle_t$ are determined by the sums of the eigenstates' components, which are added to each other with arbitrary phases. These sums are proportional to $\sqrt{\Gamma_{1,2}} P_{1,2}$, which are determined only by the eigenstates and become equal to each other above the transition point.

Note that when $t < T_R$, the phases of the eigenstates components in the sums (31) and (35) are not random, therefore, the sums are not proportional to $\sqrt{\Gamma_{1,2}} P_{1,2}$ and the dependence of $\langle |a_1| \rangle_t / \langle |a_2| \rangle_t$ on the coupling is smooth [Figure 7(b)]. Moreover, when the averaging time is much less than the return time T_R , the averaging over time does not lead to zeroing of the sign-alternating terms in the Eqns. (26), (27). This is also a reason that the dependence of $\langle |a_1| \rangle_t / \langle |a_2| \rangle_t$ on the coupling strength is smooth [Figure 7(b)].

-
- [1] L. D. Landau and E. M. Lifshitz, *Statistical Physics: Volume 5*, Vol. 5 (Elsevier, 2013).
- [2] P. W. Higgs, Broken symmetries and the masses of gauge bosons, *Phys. Rev. Lett.* **13**, 508 (1964).
- [3] P. W. Anderson, *Concepts in Solids* (Benjamin, New York, 1963) pp. 175–182.
- [4] J. Goldstone, A. Salam, and S. Weinberg, Broken symmetries, *Physical Review* **127**, 965 (1962).
- [5] L. D. Landau and E. M. Lifshitz, *Quantum mechanics: Non-relativistic theory*, Vol. 3 (Elsevier, 2013).
- [6] C. M. Bender and S. Boettcher, Real spectra in non-hermitian hamiltonians having p t symmetry, *Phys. Rev. Lett.* **80**, 5243 (1998).
- [7] N. Moiseyev, *Non-Hermitian quantum mechanics* (Cambridge University Press, 2011).
- [8] S. Klaiman, U. Günther, and N. Moiseyev, Visualization of branch points in pt-symmetric waveguides, *Phys. Rev. Lett.* **101**, 080402 (2008).
- [9] K. G. Makris, R. El-Ganainy, D. N. Christodoulides, and Z. H. Musslimani, Beam dynamics in pt symmetric optical lattices, *Phys. Rev. Lett.* **100**, 103904 (2008).
- [10] A. Guo, G. J. Salamo, D. Duchesne, R. Morandotti, M. Volatier-Ravat, V. Aimez, G. A. Siviloglou, and D. N. Christodoulides, Observation of pt-symmetry breaking in complex optical potentials, *Phys. Rev. Lett.* **103**, 093902 (2009).
- [11] C. E. Rüter, K. G. Makris, R. El-Ganainy, D. N. Christodoulides, M. Segev, and D. Kip, Observation of parity–time symmetry in optics, *Nature Phys.* **6**, 192 (2010).
- [12] A. A. Zyblovsky, A. P. Vinogradov, A. A. Pukhov, A. V. Dorofeenko, and A. A. Lisyansky, Pt-symmetry in optics, *Phys.-Usp.* **57**, 1063 (2014).
- [13] R. El-Ganainy, K. G. Makris, M. Khajavikhan, Z. H. Musslimani, S. Rotter, and D. N. Christodoulides, Non-hermitian physics and pt symmetry, *Nature Phys.* **14**, 11 (2018).
- [14] S. Longhi, Parity-time symmetry meets photonics: A new twist in non-hermitian optics, *EPL* **120**, 64001 (2018).
- [15] M.-A. Miri and A. Alù, Exceptional points in optics and

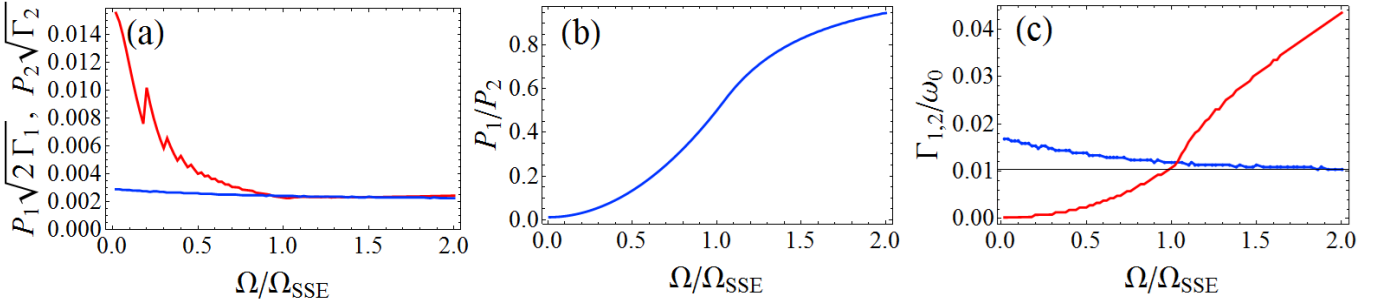


FIG. 11. (a) The dependences of $\left| \sum_{k=1}^N (e_k)_{1,2}^2 e^{i f_k t} \right|$ (the blue line) and $\left| \sum_{k=1}^N (e_k)_2^2 e^{i f_k t} \right|$ (the red line) calculated by the Eqns. (36)–(39) on the coupling strength between the oscillators. (b) The dependence of the ratio of peak heights, $P_1/P_2 = \max(e_k)_1^2 / \max(e_k)_2^2$, on the coupling strength. (c) The dependence of the peak widths, $\Gamma_{1,2}$, on the coupling strength. Γ_1 is shown by the blue line, and Γ_2 is shown by the red line.

photonics, *Science* **363**, eaar7709 (2019).

- [16] Ş. K. Özdemir, S. Rotter, F. Nori, and L. Yang, Parity-time symmetry and exceptional points in photonics, *Nature Mater.* **18**, 783 (2019).
- [17] T. T. Sergeev, A. A. Zyablovsky, E. S. Andrianov, A. A. Pukhov, Y. E. Lozovik, and A. P. Vinogradov, A new type of non-hermitian phase transition in open systems far from thermal equilibrium, *Sci. Rep.* **11**, 24054 (2021).
- [18] F. E. Öztürk, T. Lappe, G. Hellmann, J. Schmitt, J. Klaers, F. Vewinger, J. Kroha, and M. Weitz, Observation of a non-hermitian phase transition in an optical quantum gas, *Science* **372**, 88 (2021).
- [19] R. Hanai, A. Edelman, Y. Ohashi, and P. B. Littlewood, Non-hermitian phase transition from a polariton bose-einstein condensate to a photon laser, *Phys. Rev. Lett.* **122**, 185301 (2019).
- [20] A. V. Sadovnikov, A. A. Zyablovsky, A. V. Dorofeenko, and S. A. Nikitov, Exceptional-point phase transition in coupled magnonic waveguides, *Phys. Rev. Appl.* **18**, 024073 (2022).
- [21] J. B. Khurgin, Exceptional points in polaritonic cavities and subthreshold fabry-perot lasers, *Optica* **7**, 1015 (2020).
- [22] T. Gao *et al.*, Observation of non-hermitian degeneracies in a chaotic exciton-polariton billiard, *Nature* **526**, 554 (2015).
- [23] D. Zhang, X.-Q. Luo, Y.-P. Wang, T.-F. Li, and J. Q. You, Observation of the exceptional point in cavity magnon-polaritons, *Nature Commun.* **8**, 1 (2017).
- [24] H. Xu, D. Mason, L. Jiang, and J. G. E. Harris, Topological energy transfer in an optomechanical system with exceptional points, *Nature* **537**, 80 (2016).
- [25] J. Zhang, B. Peng, Ş. K. Özdemir, K. Pichler, D. O. Krimer, G. Zhao, F. Nori, Y.-X. Liu, S. Rotter, and L. Yang, A phonon laser operating at an exceptional point, *Nature Photon.* **12**, 479 (2018).
- [26] Y.-H. Lai, Y.-K. Lu, M.-G. Suh, Z. Yuan, and K. Vahala, Observation of the exceptional-point-enhanced sagnac effect, *Nature* **576**, 65 (2019).
- [27] H. Hodaei, A. U. Hassan, S. Wittek, H. Garcia-Gracia, R. El-Ganainy, D. N. Christodoulides, and M. Khajavikhan, Enhanced sensitivity at higher-order exceptional points, *Nature* **548**, 187 (2017).
- [28] W. Chen, Ş. K. Özdemir, G. Zhao, J. Wiersig, and L. Yang, Exceptional points enhance sensing in an optical microcavity, *Nature* **548**, 192 (2017).
- [29] J. Wiersig, Enhancing the sensitivity of frequency and energy splitting detection by using exceptional points: application to microcavity sensors for single-particle detection, *Phys. Rev. Lett.* **112**, 203901 (2014).
- [30] A. A. Zyablovsky, I. V. Daronin, E. S. Andrianov, A. A. Pukhov, Y. E. Lozovik, A. P. Vinogradov, and A. A. Lisyansky, Exceptional points as lasing prethresholds, *Laser Photonics Rev.* **15**, 2000450 (2021).
- [31] H. Hodaei, M.-A. Miri, M. Heinrich, D. N. Christodoulides, and M. Khajavikhan, Parity-time-symmetric microring lasers, *Science* **346**, 975 (2014).
- [32] B. Peng, Ş. K. Özdemir, M. Liertzer, W. Chen, J. Kramer, H. Yilmaz, J. Wiersig, S. Rotter, and L. Yang, Chiral modes and directional lasing at exceptional points, *Proc. Natl. Acad. Sci. USA* **113**, 6845 (2016).
- [33] I. V. Daronin, A. A. Zyablovsky, E. S. Andrianov, A. A. Pukhov, and A. P. Vinogradov, Lasing without inversion due to parametric instability of the laser near the exceptional point, *Phys. Rev. A* **100**, 021801(R) (2019).
- [34] I. V. Daronin, A. A. Zyablovsky, and E. S. Andrianov, Strong-coupling-assisted formation of coherent radiation below the lasing threshold, *Opt. Express* **29**, 5624 (2021).
- [35] G.-Q. Zhang and J. Q. You, Higher-order exceptional point in a cavity magnonics system, *Phys. Rev. B* **99**, 054404 (2019).
- [36] Z.-P. Liu, J. Zhang, Ş. K. Özdemir, B. Peng, H. Jing, X.-Y. Lü, C.-W. Li, L. Yang, F. Nori, and Y.-X. Liu, Metrology with pt-symmetric cavities: enhanced sensitivity near the pt-phase transition, *Phys. Rev. Lett.* **117**, 110802 (2016).
- [37] L. Feng, Z. J. Wong, R.-M. Ma, Y. Wang, and X. Zhang, Single-mode laser by parity-time symmetry breaking, *Science* **346**, 972 (2014).
- [38] M. Liertzer, L. Ge, A. Cerjan, A. D. Stone, H. E. Türeci, and S. Rotter, Pump-induced exceptional points in lasers, *Phys. Rev. Lett.* **108**, 173901 (2012).
- [39] S. Longhi, Bloch oscillations in complex crystals with p t symmetry, *Phys. Rev. Lett.* **103**, 123601 (2009).
- [40] S. V. Suchkov, A. A. Sukhorukov, J. Huang, S. V. Dmitriev, C. Lee, and Y. S. Kivshar, Nonlinear switching and solitons in pt-symmetric photonic systems, *Laser Photonics Rev.* **10**, 177 (2016).

- [41] M. O. Scully and M. S. Zubairy, *Quantum optics* (1999).
- [42] A. O. Caldeira and A. J. Leggett, Path integral approach to quantum brownian motion, *Physica A: Statistical mechanics and its Applications* **121**, 587 (1983).
- [43] U. Weiss, *Quantum dissipative systems* (World Scientific, 2012).
- [44] I. De Vega and D. Alonso, Dynamics of non-markovian open quantum systems, *Rev. Mod. Phys.* **89**, 015001 (2017).
- [45] H. Carmichael, *An open systems approach to quantum optics: lectures presented at the Université Libre de Bruxelles, October 28 to November 4, 1991*, Vol. 18 (Springer Science & Business Media, 2009).
- [46] C. Gardiner and P. Zoller, *Quantum noise: a handbook of Markovian and non-Markovian quantum stochastic methods with applications to quantum optics* (Springer Science & Business Media, 2004).
- [47] C. M. Bender, S. Boettcher, and P. N. Meisinger, P-t-symmetric quantum mechanics, *J. Math. Phys.* **40**, 2201 (1999).
- [48] H. Yuan, Y. Cao, A. Kamra, R. A. Duine, and P. Yan, Quantum magnonics: When magnon spintronics meets quantum information science, *Physics Reports* **965**, 1 (2022).
- [49] X.-g. Wang, D. Schulz, G.-h. Guo, and J. Berakdar, Magnon dynamics in parity-time-symmetric dipolarly coupled waveguides and magnonic crystals, *Phys. Rev. Appl.* **18**, 024080 (2022).
- [50] M. Jack, M. Collett, and D. Walls, Coherent quantum tunneling between two bose-einstein condensates, *Phys. Rev. A* **54**, R4625 (1996).
- [51] F. Trimborn, D. Witthaut, and S. Wimberger, Mean-field dynamics of a two-mode bose-einstein condensate subject to noise and dissipation, *J. Phys. B* **41**, 171001 (2008).
- [52] E.-M. Graefe, Stationary states of a p-t symmetric two-mode bose-einstein condensate, *J. Phys. A* **45**, 444015 (2012).
- [53] V. V. Konotop, J. Yang, and D. A. Zezyulin, Nonlinear waves in p-t-symmetric systems, *Rev. Mod. Phys.* **88**, 035002 (2016).
- [54] H.-P. Breuer, E.-M. Laine, J. Piilo, and B. Vacchini, Colloquium: Non-markovian dynamics in open quantum systems, *Rev. Mod. Phys.* **88**, 021002 (2016).
- [55] V. I. Tatarskii, Example of the description of dissipative processes in terms of reversible dynamic equations and some comments on the fluctuation-dissipation theorem, *Soviet Physics Uspekhi* **30**, 134 (1987).
- [56] B. Kolaric, B. Maes, K. Clays, T. Durt, and Y. Caudano, Strong light-matter coupling as a new tool for molecular and material engineering: Quantum approach, *Advanced Quantum Technologies* **1**, 1800001 (2018).
- [57] A. Pikovsky, M. Rosenblum, and J. Kurths, *Synchronization. A universal concept in nonlinear sciences* (Cambridge University Press, 2001).
- [58] J. Plemelj, *Problems in the sense of Riemann and Klein* (Interscience Publishers, 1964).
- [59] T. T. Sergeev, I. V. Vovcenko, A. A. Zyablovsky, and E. S. Andrianov, Environment-assisted strong coupling regime, *Quantum* **6**, 684 (2022).
- [60] V. V. Petrov, *Sums of independent random variables* (Springer-Verlag, New York-Heidelberg, 1976).
- [61] Z. Lin, H. Ramezani, T. Eichelkraut, T. Kottos, H. Cao, and D. N. Christodoulides, Unidirectional invisibility induced by p-t-symmetric periodic structures, *Phys. Rev. Lett.* **106**, 213901 (2011).